BBA - General Subjects 1865 (2021) 129732

Contents lists available at ScienceDirect

BBA - General Subjects

journal homepage: www.elsevier.com/locate/bbagen

Understanding the role of apolipoproteinA-I in atherosclerosis. Post-translational modifications synergize dysfunction?

Ivo Díaz Ludovico[a,b,1], Romina A. Gisonno[a,b,1], Marina C. Gonzalez[a,b], Horacio A. Garda[a,b], Nahuel A. Ramella[a,b,*], M. Alejandra Tricerri[a,b,*]

[a] Instituto de Investigaciones Bioquímicas de La Plata (INIBIOLP), Argentina
[b] Facultad de Ciencias Médicas, Universidad Nacional de La Plata, Calle 60 y 120, La Plata CP 1900, Argentina

ARTICLE INFO

Keywords:
Atherosclerosis
Apolipoprotein A-I
K107del natural variant
Protein misfolding
Amyloidosis
Inflammation

ABSTRACT

Background: The identification of dysfunctional human apolipoprotein A-I (apoA-I) in atherosclerotic plaques suggests that protein structure and function may be hampered under a chronic pro inflammatory scenario. Moreover, the fact that natural mutants of this protein elicit severe cardiovascular diseases (CVD) strongly indicates that the native folding could shift due to the mutation, yielding a structure more prone to misfold or misfunction. To understand the events that determine the failure of apoA-I structural flexibility to fulfill its protective role, we took advantage of the study of a natural variant with a deletion of the residue lysine 107 (K107del) associated with atherosclerosis.

Methods: Biophysical approaches, such as electrophoresis, fluorescence and spectroscopy were used to characterize proteins structure and function, either in native conformation or under oxidation or intramolecular crosslinking.

Results: K107del structure was more flexible than the protein with the native sequence (Wt) but interactions with artificial membranes were preserved. Instead, structural restrictions by intramolecular crosslinking impaired the Wt and K107del lipid solubilization function. In addition, controlled oxidation decreased the yield of the native dimer conformation for both variants.

Conclusions: We conclude that even though mutations may alter protein structure and spatial arrangement, the highly flexible conformation compensates the mild shift from the native folding. Instead, post translational apoA-I modifications (probably chronic and progressive) are required to raise a protein conformation with significant loss of function and increased aggregation tendency.

General significance: The results learnt from this variant strength a close association between amyloidosis and atherosclerosis.

1. Introduction

An extensive research field supports a key role of human high density lipoproteins (HDL) and their major protein apolipoprotein A-I (apoA-I) in the protection against cardiovascular disease [1,2]. An overall agreement highlights their beneficial participation in the reverse cholesterol transport (RCT), which delivers excess of cholesterol from peripheral cells to the liver for its catabolism [3]. In addition, it has been recognized the crucial participation of HDL and apoA-I in pathways protecting endothelial functions: stimulation of nitric oxide-mediated vasodilatation [4], reduction of vascular cell adhesion molecule-1 (VCAM-I) expression [5,6], and inhibition of apoptosis promoting proliferation [7]. The multiple functions of apoA-I have been extensively related to its highly flexible structure. Also, a dynamic interconversion between lipid-free and lipid-bound states mediates its efficiency to interact with membranes and recruit phospholipids and cholesterol. Most of the protein circulates bound as complex HDL particles, and a minor fraction, about 5% is recycled as the lipoprotein is catabolized, yielding lipid-free or lipid-poor conformations which are more effective to interact with key proteins such as ATP-binding cassette proteins A1 and G1 (ABCA1 and ABCG1 receptors) and lecithin: cholesterol acyltransferase (LCAT) ([8] and references described there). Moreover, many other functions of apoA-I have been identified *in vitro,* suggesting that the protein mimics some of the pathways observed for

* Corresponding authors.
E-mail addresses: nramella@med.unlp.edu.ar (N.A. Ramella), aletricerri@med.unlp.edu.ar (M.A. Tricerri).
[1] Contributed equally to this work.

https://doi.org/10.1016/j.bbagen.2020.129732
Received 7 June 2020; Received in revised form 17 August 2020; Accepted 9 September 2020
Available online 15 September 2020

HDL, as decreasing the respiratory burst induced by oxidized low density lipoproteins (oxLDL) [9] and binding to bacterial lipopolysaccharide (LPS) [10,11].

Despite the aforementioned information, the "HDL-cholesterol hypothesis" has been revised as it seemed to be oversimplified by setting an atherosclerosis-risk index from LDL/HDL ratio [8,12]. Beyond the usefulness of this ratio as a clinical parameter, atherosclerosis is a complex chronic pathological scenario, becoming a pro-oxidant environment with the release of reactive oxygen species (ROS) related to the failure of cholesterol homeostasis Thereby, quality of lipoproteins is considered to be a good predictor in addition to their quantity. Atherosclerotic plaques are characterized by dysfunctional apoA-I aggregated in the artery walls [13]. Protein distribution in human aorta is quite different from the circulating conformations. It is identified in high amounts deposited in chronic lesions predominantly lipid-poor, not associated with HDL, extensively oxidized and cross-linked, and functionally impaired [14]. Whether protein misfolding is a cause or a consequence of this microenvironment is not known. In this regard, it was shown the presence of diffuse deposits of apoA-I as amyloid patches in complicated atherosclerotic plaques [15]. This fact indicates that amyloidosis and atherosclerosis may be closely associated [16].

About twenty natural variants of apoA-I have been described inducing amyloidosis with deposit and failure of target organs such as heart, liver or kidney [17]. Interestingly, one naturally occurring deletion variant (K107del) was described inducing a unique pathologic pattern, as amyloidosis was associated with severe atherosclerosis [18]. The facts that determine this behavior are far to be known. The loss of function the increased tendency to misfold, or the ability to elicit a pro inflammatory environment were suggested to mediate its role in these diseases [19]. Taking advantage of the structural comparative study among K107del and the protein with the native sequence (Wt), we proposed here to understand the reasons that may affect apoA-I misfunction and aggregation in the atherosclerotic plaques. Deep structural knowledge of this variant may help clarify the participation of apoA-I (or its failure to fulfill the protective roles). As oxidation and crosslinking events are present in atherosclerotic plaques, we analyzed the variant's natural flexibility and function under native conditions and under controlled chemical modifications that could mimic those undergoing in a chronic pathological scenario.

2. Materials and methods

2.1. Materials

Guanidine hydrochloride (GndHCl), thioflavin T (ThT), cholesterol (Chol), sodium cholate, ethylenediaminetetraacetic acid (EDTA), sodium chloride (NaCl), sodium dodecyl sulfate (SDS),Terbium -III chloride (Tb) and dipicolinic acid (DPA) were from Sigma-Aldrich (St Louis, MO); 1-palmitoyl-2-oleoylphosphatidylcholine (POPC) and dimyristoylphosphatidylcholine (DMPC) were purchased from Avanti Polar Lipids (Alabaster, AL); His-purifying resin was from Novagen (Darmstadt, Germany). Bis-(sulfosuccinimidyl) suberate (BS^3) and isopropyl-β-D-thiogalactoside (IPTG) were purchased to Thermo Scientific (Waltham, MA). All other reagents were of the highest analytical grade available.

2.2. Cloning, expression and purification of wild-type and K107del apoA-I

Proteins were expressed as previously described in [20,21]. The cDNA of apoA-I with the native sequence (Wt) and K107del were modified to introduce an acid labile Asp-Pro peptide bond between amino acid residues 2 and 3 of apoA-I, which allowed specific chemical cleavage of an N-terminal His-Tag fusion peptide. These constructs, inserted into a pET-30 plasmid (Novagen, Madison, WI), were transformed into BL21 (DE) *Escherichia coli* cells (Novagen, Madison, WI), then expressed by induction with IPTG and purified by elution through Ni-chelating columns (Novagen, Madison, WI) as described [21]. This resulted in a high yield of protein with a purity of at least 95% (determined by SDS-PAGE).

2.3. Crosslinking of proteins

Proteins were crosslinked at 0.05 mg/mL in PBS pH 7.9 for 3 h without agitation at room temperature. Fresh BS^3 was added (within 1 min after solubilization in PBS to avoid hydrolysis of free crosslinker) at 30:1 BS^3:protein molar ratio [22]. Reactions were quenched after 15 min by the addition of Tris buffer to a final concentration of 50 mM. The concentration of crosslinked proteins was calculated by the BCA Protein Assay Kit (Thermo Scientific (Waltham, MA)). The presence of the monomeric conformation after the treatments was confirmed by polyacrylamide gradient electrophoresis, either under native or denaturing conditions. In order to evaluate whether protein oxidation may induce an aggregation prone conformation, proteins were incubated for 24 h at 0.5 mg/mL and crosslinked as described above.

2.4. Protein oxidation

Wt and K107del were chemically oxidized by overnight incubation in a 10,000 M excess of H_2O_2 at 37 °C for 12 h. The concentration of H_2O_2 was determined spectrophotometrically (ε 39.4 M^{-1} cm^{-1} at 240 nm) [23]. Excess of H_2O_2 was removed by extensive dialysis against 10 mM sodium phosphate buffer pH 6.0 (fibrillation buffer). Molecular weights (Mw) of Wt and K107del oxidized proteins were calculated by intact protein mass spectrometry analysis. This analysis was performed at the Proteomics Core Facility CEQUIBIEM, at the University of Buenos Aires/CONICET (National Research Council). Samples were analyzed using an Ultraflex II Bruker Daltonics UV-MALDI-TOF-TOF mass spectrometer. Spectra were obtained in positive linear mode (LP), within a mass range of 20,000–60,000 *m/z*. The generated spectra were visualized and compared with FlexAnalysis 3.3 software.

2.5. Fluorescence measurements

Tryptophan (Trp) intrinsic fluorescence emission spectra were acquired on an Olis upgraded SLM4800 spectrofluorometer (ISS Inc., Champaign, IL). Proteins, either freshly resuspended or after chemical modifications were diluted to 0.05–0.2 mg/mL in Tris 20 mM pH 7.4 or PBS at the same pH. Excitation wavelength was fixed at 295 nm as previously registered [21,24].

2.6. Protein/lipids interaction methodologies

2.6.1. Unilamellar liposomes construction

One mg of POPC or (POPC:Chol at a 4:1 M ratio) from a stock solution in chloroform was used to form a film in a round-bottom tube, dried by blowing a N_2 atmosphere and exhaustively exposed to vacuum in a lyophilizer (Virtis) to evaporate the solvent. Then, the fluorescent complex [Tb-DPA] was achieved by the addition of 15 mM Tb and 150 mM DPA in 10 mMTris pH 8.0 added to final concentration 1 mg/mL of lipids. Multilamellar liposomes (MLV) were attained by extensive vortexing, followed by sonication to rearrange lipids into small unilamellar vesicles (SUVs). Excess of the fluorescent complex was removed by elution of the SUVs through a Superose 6 HR 10/30 column (Pharmacia) equilibrated and eluted with 10 mM Tris pH 8.0, 150 mM NaCl and 12.5 mM EDTA [25,26]. Only fractions showing the highest fluorescence yield were used within 5–7 days.

2.6.2. Leakage measurements

SUVs were added into the cuvette with proteins at 0.3 mg/mL, and homogenized by rapid pipetting (about 5 s. per sample). Then, time-dependent fluorescence intensity was followed for 10 min with

excitation and emission fixed at 250 and 544 nm, respectively. Leakage efficiency was calculated as a percentage of the decrease in fluorescence intensity (F) with respect to the initial value (Fo). The decrease of fluorescence induced by the addition of 1% SDS (Fo-Ft) was taken as a 100% leakage [25,26]. Results are shown as triplicates of 3 different experiments.

2.6.3. Clearance measurement

To obtain MLV of DMPC, lipids from a stock solution in chloroform were dried under N_2 flux as explained above, and resuspended in Tris buffer pH 7.4 to a final DMPC concentration of 5 mg/mL. The tube was vortexed at room temperature for 5 min, heating at 37 °C in 30-s cycles. DMPC vesicles were added to the 0.05 mg/mL proteins samples until a final molar ratio of 145:1 DMPC:protein. Samples were gently mixed (for 5 s.) and clearance was determined by monitoring Optical Density (DO) at 325 nm and 24 °C in a Beckman Coulter DTX 880 Microplate Reader (Beckman, CA). All DMPC experiments were performed in the presence of 0.05% sodium azide. Curves were adjusted by fitting to a single exponential decay $y = y_0 + ae^{-bx}$. Next, the characterization of the final product was attained by 4–30% home-made native PAGGE developed with silver staining. The relative amount of the populations achieved for each variant was estimated by quantifying with the Image J 1.51 j8 software the associated intensity of the protein within each band. The relative size of the particles was also estimated by size exclusion chromatography (SEC) using a Merck-Hitachi L6200 Intelligent pump. Samples were eluted through the Superose 6 HR 10/30 column, equilibrated with 50 mM Tris buffer pH 7.4 at a flow of 0.5 mL/min, and detected at 280 nm using a UV-VIS detector (Merck-Hitachi L4200). Particle morphology was characterized by transmission electron microscopy (TEM) on a JEOL-1200 EX. Samples were seeded on Formvard grids, contrasted with 0.5% phosphotungstic acid and visualized by negative staining.

2.7. Other analytical methods

Spatial arrangement of K107del was modeled using the SWISS-MODEL server (https://swissmodel.expasy.org, Swiss Institute of Bioinformatics Biozentrum, University of Basel Klingelbergstrasse, Basel, Switzerland) using the alignment model [27] with the apoA-I structural template obtained by Melchior et al. [28]. Protein structure figures and homology models were generated using UCSF Chimera, developed by the UCSF Resource for Biocomputing [29]. For most of the experiments, protein content was quantified by the Bradford technique [30]. For statistical analysis, datasets were analyzed in GraphPad Prism 8.0 software using unpaired parametric test. Only results with a confidence level of $p < 0.05$ were considered. Unless otherwise stated, results either of biophysical or biological assays were reproduced in three independent experiments and were indicated as means of triplicates ± standard deviation. Statistically significant differences between experimental conditions were evaluated by ANOVA or the Student's test.

3. Results

3.1. Proteins purification

ApoA-I variants (either Wt or K107del) were isolated and purified from bacterial strains in high yield and purity (Suppl Fig. 1). We have previously shown that Wt purified under this protocol behaves almost indistinguishable from plasma apoA-I [20].

3.2. Leakage

In order to characterize the influence of the deletion of the positive Lys residue in position 107 on protein function, we first compared the interaction of the variant with lipid bilayers, monitoring protein-induced leakage of SUVs. Energy transfer from DPA to Tb is highly efficient in the complex confined to the vesicles internal aqueous space. If apoA-I-induced leakage occurs, excess of EDTA present in the medium replaces DPA in the complex and fluorescence decreases. As previously observed, membrane disruption mediated by Wt was smooth and slow [26] (Figure1A and B).

In order to compare both variants, leakage extension induced by freshly folded Wt and K107del was evaluated after 10-min interaction. As Fig. 1C shows, no differences were detected among both variants in their capacity to induce membrane permeation. Although a higher tendency to leakage was observed from vesicles containing Chol, the effect was neither significant nor different among variants, even at the different protein ratios tested (not shown).

3.3. Protein chemical treatments. Oxidation and crosslinking

3.3.1. Protein structure

BS^3 crosslinker has been widely used for the analysis of apoA-I structure [22]. Its short spacer arm (~11 Å) makes it suitable to covalently fix primary amine groups within proteins. In addition to the N terminal amine group, apoA-I contains a high number of Lys residues which may be exposed to interact with the reagent in an aqueous solvent. To compare the relative efficiency of K107del to crosslink, we first diluted proteins at 0.5 mg/mL. Under these conditions and in agreement with previous reports, Wt showed some degree of dimers covalently fixed (lane 4 in Fig. 2A). This effect is less evident for the deletion mutant (lane 5). Afterwards, we set to determine the structural effect that may occur if crosslinking was restricted to intra-chain bonds. In this trend, proteins were set at 0.05 mg/mL, as classic studies have shown mainly monomer conformation present under that concentration [22,31], and following crosslinking protein mobility was compared by gradient gel electrophoresis under native conditions (PAGGE). As Fig. 2B shows, only monomeric species were attained. However, the efficiency of crosslinking was evident as treated proteins migrated slightly but significantly faster than the untreated ones. This observation may be explained by either a more compact conformation of crosslinked proteins, and/or by a gain in the net negative charge due to the crosslinker interaction with Lys residues.

In order to compare whether oxidized proteins should keep the ability to self-associate, variants (either non-oxidized or after incubation with H_2O_2) were incubated at 0.5 mg/mL for 24 h at pH 6.0, then taken to pH 7.9, and further treated with BS^3 as previously described (section 2.3). As it may be observed in Fig. 2C, the band corresponding to dimer was vanished for the oxidized species, indicating a loss in the oligomerization capability.

The relative exposition of the Trp residues to the solvent may be used as a conformational control of protein arrangement, as it is well known that the high flexibility of apoA-I may be censored from the shift in the intrinsic fluorescence. By fixing excitation wavelength at 295 nm, fluorescence is dominated in average by four Trp residues (in positions 8, 50, 72 and 108 in the native sequence) [24,32]. In agreement with previous reported results [32,33] the wavelength of maximum fluorescence of Trp (WMF) in the freshly folded K107del variant showed a small but significant 2 nm-shift to the red with respect to Wt. BS^3-crosslinking did not introduce a significant structural modification as compared with uncrosslinked species either for Wt or K107del (Fig. 3A and B respectively).

Afterwards, we analyzed the effect of oxidation on protein structure. We have previously described that treatment with controlled H_2O_2 resulted in the preservation of mainly the protein molecular weight integrity but, as expected, it induced a mild tendency to oligomerize [19,34]. To further test whether aromatic residues could be affected during H_2O_2 oxidation, we checked intrinsic fluorescence of the oxidized variants. About 4 nm-shift to the red of the WMF and a small decrease in intensity indicated that the aromatic residues are relatively more exposed in both variants but significantly preserved, as extensive

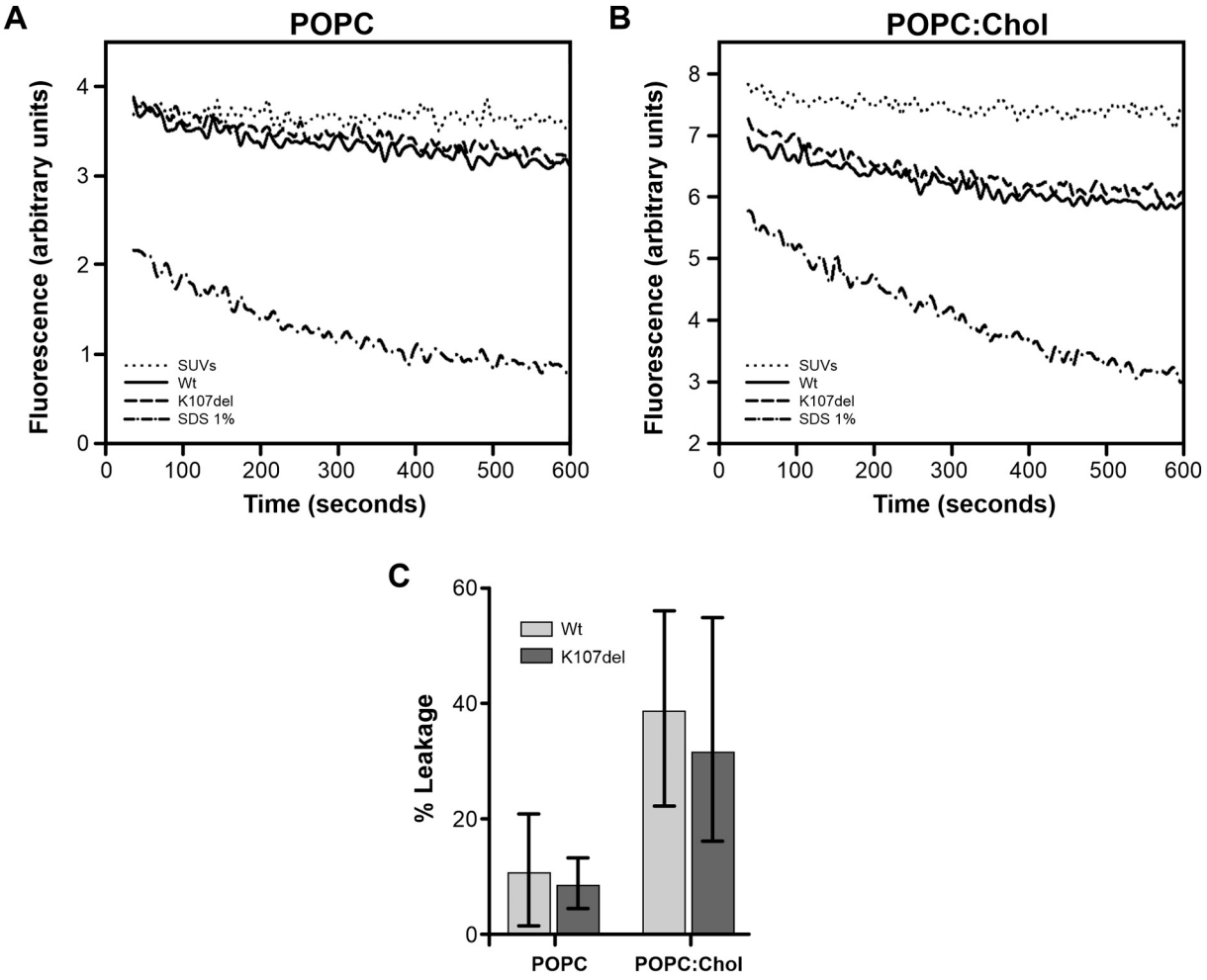

Fig. 1. Leakage induced by Wt and K107del of Tb/DPA-loaded lipid vesicles. A) and B), time dependence of the fluorescence intensity change obtained by adding 0.3 mg/mL of Wt or K107del to A) POPC or B) POPC:Chol SUVs. Fluorescence was registered with excitation set at 250 and emission at 544 nm. C) Percentage of leakage was calculated to the final point (last 60 s.) after 600-s. interaction. One-hundred % was taken as the decrease of fluorescence after addition of 1% SDS (dashed-point line in Fig. A and B). Bars represent media ± standard deviation of triplicates of three independent measurements. No differences were found between all conditions by evaluation by *t*-test ($p \leq 0.05$).

oxidation should result in a significant decrease in the quantum yield (Fig. 3C and D).

Fluorescence was measured in an SLM 4800 spectrofluorometer fixing excitation wavelength at 295 nm and monitoring emission from 310 to 400 nm. **A)** Wt and **B)** K107del at 0.05 mg/mL in PBS pH 7.9 buffer either before (continuous lines) or after crosslinking (pointed lines). Spectra were normalized to the highest intensity to better compare the shift in the fluorescence emission. **C)** Wt and **D)** K107del intrinsic fluorescence registered before (continuous lines) or after oxidative treatment (dashed lines).

In order to evaluate oxidization of K107del comparatively to Wt, we measured the intact mass of both non-oxidized and oxidized apoA-I variants through mass spectrometry (Fig. 4). Mw obtained for oxidized Wt (Fig. 4A, 27,857 Da) or K107del (Fig. 4B, 27,727 Da) was each 71 Da-higher than the values obtained for the native variants [19]. Taking into account that sodium adducts can add +23 Da, this change in molecular weight is compatible with the complete oxidation of all methionine residues, already described for apoA-I [34,35]. The same global mass gain would suggest that both proteins are undergoing equivalent oxidative processes. In addition of a main peak corresponding to the monomer, a small peak of 56 kDa may indicate a small amount of Wt dimer present in the sample (inset Fig. 4A).

3.3.2. *Effect of chemical modification on protein function*

With the aim of answering whether chemical modifications may affect proteins function, we performed a well-established test, as it is the ability of apoA-I to solubilize lipids from vesicles at the lipids transition temperature [24]. Fig. 5A shows that, in agreement with leakage experiments, the deletion of Lys107 did not modify the protein's efficiency to interact with DMPC. Chemical modification of proteins by oxidation reflects a similar result showing no significant differences to solubilize lipids between the oxidized Wt and K107del. However, oxidized proteins presented an increased capacity to clarify MLV liposomes with respect to the native protein conformations. Evaluation of the structural restriction induced by intramolecular crosslinking resulted in drastic impairment of the variants´ ability to induce clearance, Wt being more affected than K107del. Significant differences in the clearance at the final point are compared in Fig. 5B.

In order to evaluate the effect of the mutation on the protein arrangement, particle morphology was characterized at the end of incubation time (Suppl Fig. 2). Under this molar lipid:apoA-I ratio most of the protein, either Wt or Lys107del, rearranged into two-discrete HDL-like complexes of molecular weight around 500 and 300 kDa, as indicated by native PAGGE and size exclusion chromatography (Suppl Fig. 2A). As suggested from both methodologies, a higher amount of apoA-I was combined in larger particles for both proteins (Suppl Fig. 2B). TEM images showed the classic disc-shaped populations

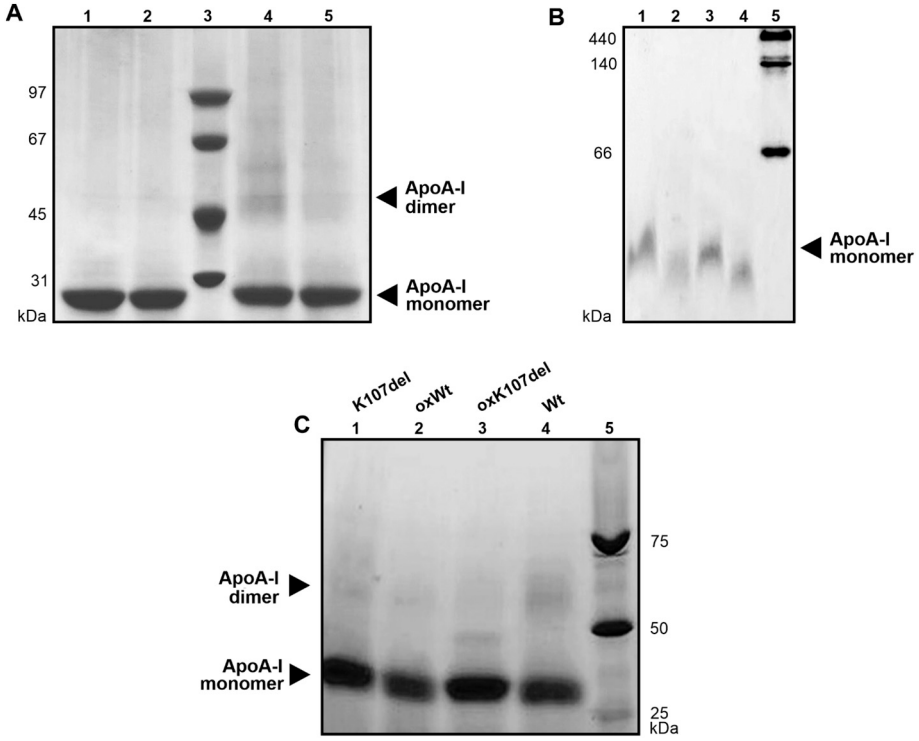

Fig. 2. Characterization of protein crosslinking by polyacrylamide gel electrophoresis. Gels were run as described and stained with Coomasie Blue. A) SDS PAGE at 16% of native or crosslinked proteins at 0.5 mg/mL. Lane 1 (Wt) and lane 2 (K107del)) before treatment with BS^3; lanes 4 and 5, Wt and K107del after crosslinking, respectively. Lane 3 shows SDS low molecular weight marker. Dark arrows indicate the Mw expected for the apoA-I monomer and dimer; B) Native PAGGE (10–20%) of proteins crosslinked at 0.05 mg/mL. Lanes 1 and 2, Wt before or after crosslinking, respectively. Lanes 3 and 4, K107del before or after crosslinking respectively. Lane 5 shows commercial high molecular weight standard; C) SDS-PAGGE (4–16%) to compare the effect of oxidation on the crosslinking efficiency. Lane 1 and 4 K107del and Wt treated with BS^3 respectively. Lanes 2 and 3 correspond to oxidized Wt and K107del treated with BS^3. Lane 5: Mw standard marker. (For interpretation of the references to colour in this figure legend, the reader is referred to the web version of this article.)

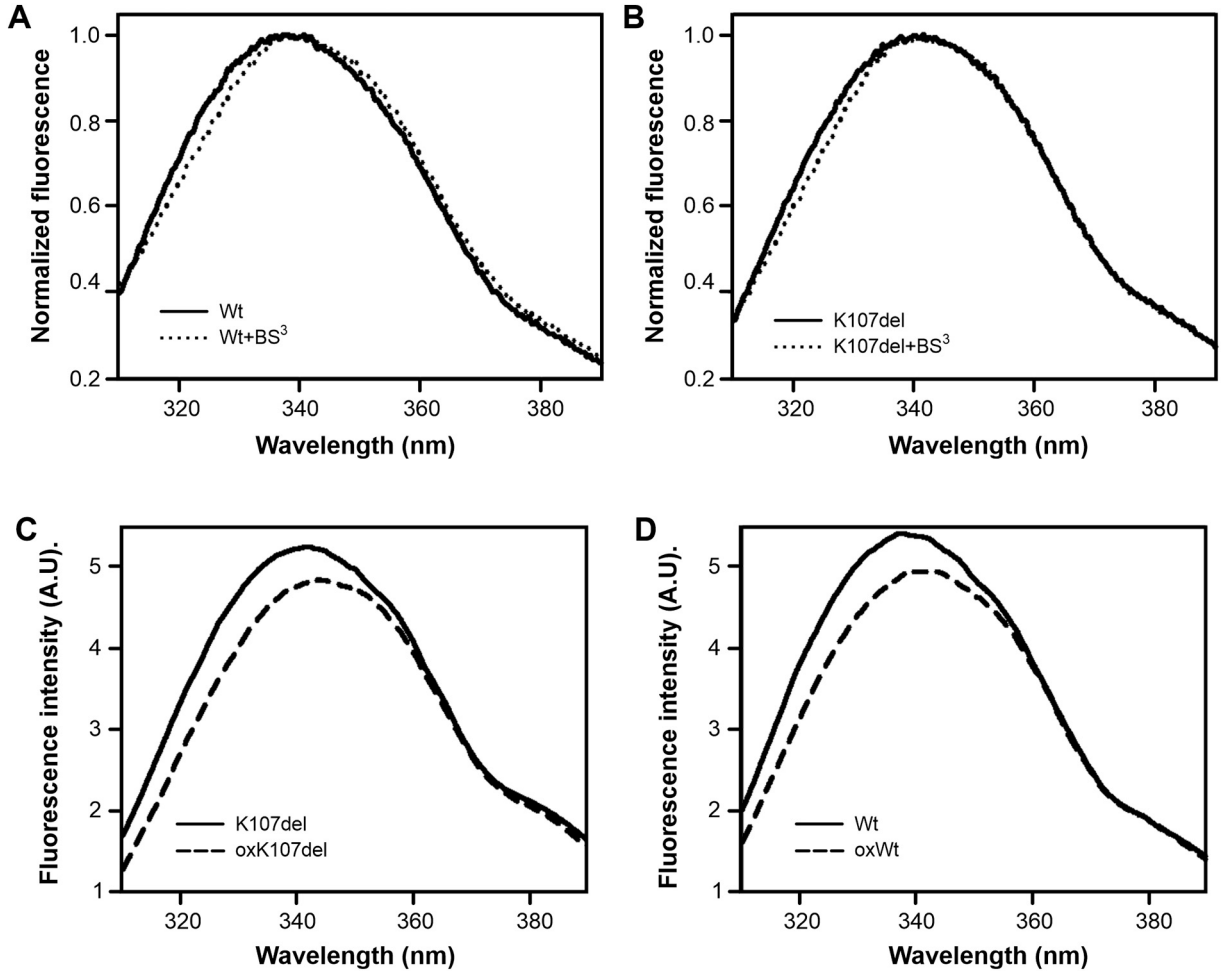

Fig. 3. Intrinsic fluorescence spectra of post-translational chemical modification of apoA-I variants.

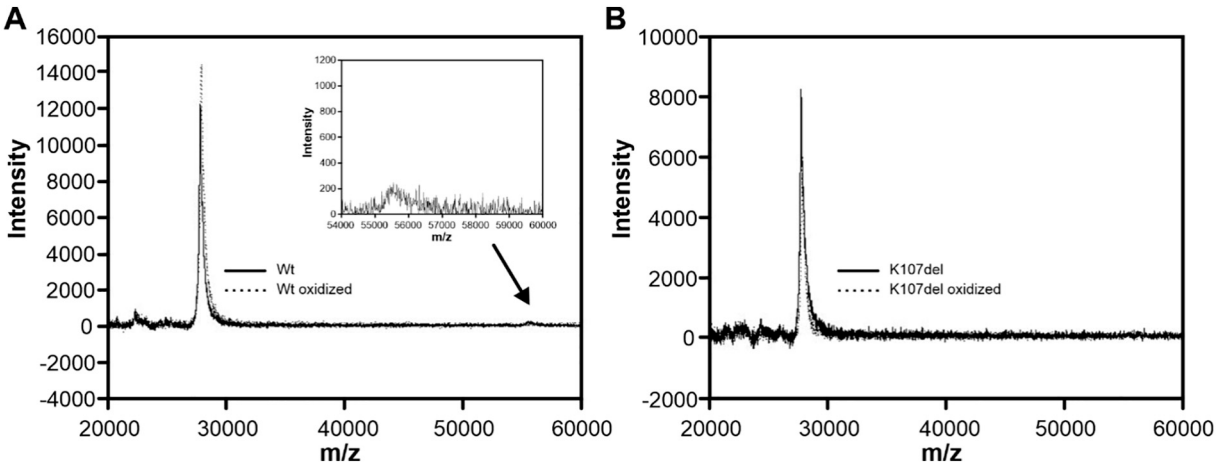

Fig. 4. Effect of oxidation on protein molecular weight. MS spectra of A) Wt and oxidized Wt and B) K107del and oxidized K107del. Inset in Fig. A) amplification of the peak shown by the black arrow, indicative of dimeric apoA-I.

(Suppl Fig. 2C). Unluckily, these images did not allow to discriminate their different size. Finally, and in order to better estimate a possible explanation for the behavior of K107del with respect to Wt, we built a model of the variant using as a template the recent consensus structure of the monomeric human apoA-I proposed from combined biophysical evidences [28]. As Fig. 6 indicates, our modeling predicts a distortion of helix 4 due to the deletion, which may weaken inter chain salt bridge interactions between neighbor glutamate and lysine residues. The estimation of solvent accessible surface area (SASA) was performed by the PyMOL Molecular Graphics System, Version 2.0 (Schrodinger, LLC), indicating a relative increase of the area exposed for K107del (15,936 $Å^2$) with respect to the Wt (15,651 $Å^2$).

4. Discussion and conclusions

In the present study, we set out to characterize local conditions that may shift apoA-I structure from the native folding, inducing its aggregation and dysfunction in the atherosclerotic plaques. From the analysis of this chronic pro inflammatory scenario, common factors are to be considered: 1) chemical modifications due to reactive oxygen species (ROS) freed by activated macrophages, among those oxidation and crosslinking [34]; 2) intrinsic modifications caused by hereditary mutations in the apoA-I sequence which should turn it prone to misfold or misfunction. In this trend the deletion mutant K107del was identified as a good target, as it was associated with severe atherosclerosis in

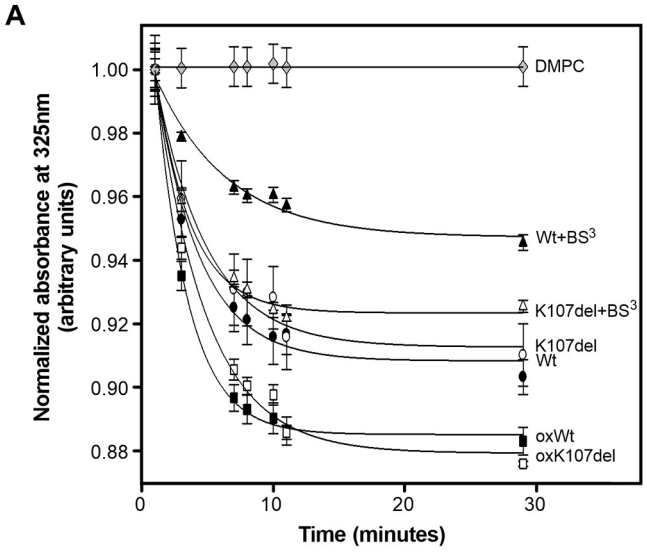

Fig. 5. Time-course of the interaction of native, crosslinked or oxidized variants with DMPC liposomes. A) Multilamellar DMPC vesicles were added to apoA-I variants at 0.05 mg/mL, to a final molar ratio of 145:1 phospholipid to protein at 24 °C. Lipid solubilization efficiency was measured by following Absorbance at 325 nm. Continuous lines correspond to the fitting of the curves to single exponential decay. B) Difference among the sample's absorbance at the last incubation time (30 min) was estimated by the *t*-test ($p \leq 0.05$).

B **Significative differences of absorbance at final point**

Protein	Wt	K107del	Wt+BS^3	K107del+BS^3	oxWt	oxK107del
Wt		**No**	Yes	Yes	Yes	Yes
K107del			Yes	**No**	Yes	Yes
Wt+BS^3				Yes	Yes	Yes
K107del+BS^3					Yes	Yes
oxWt						**No**
oxK107del						

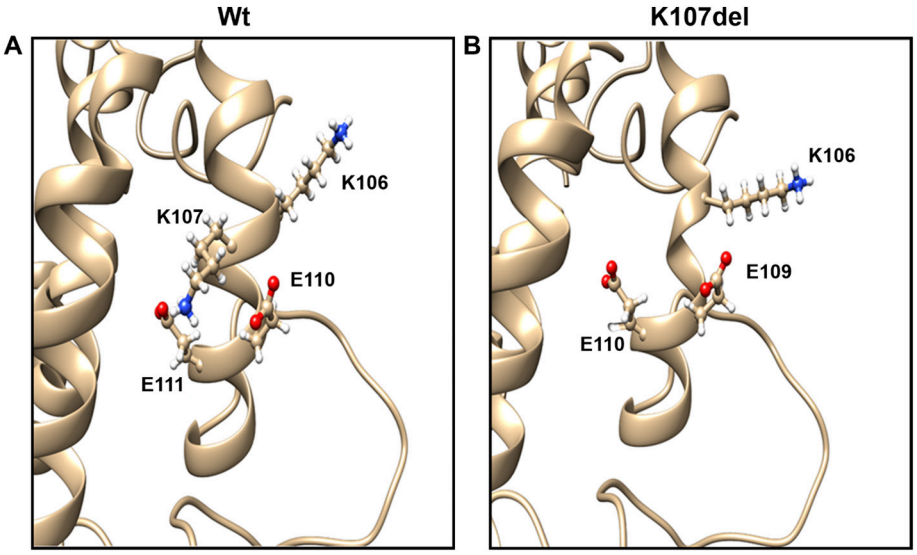

Fig. 6. Model of the apoA-I Wt and K107del structural arrangement. Crystallographic structure of A) apoA-I Wt or B) K107del modeled using the SWISS-MODEL server (https://swissmodel.expasy.org), with the apoA-I structural template obtained from Melchior et al. [28]. Protein main chain is shown in ribbon diagram. Both images show the amino acids lysine and glutamate in the form of balls and sticks.

patients [36,37]. Studies performed in *in vitro* and *in vivo* models have not completely determined either the reasons for the failure of apoA-I to fulfill the atheroprotective role or the increment in the severity of the lesions linked to the deletion variant.

Although lower-than-normal levels of HDL were usually attributed to the phenotype of patients carrying apoA-I K107del [36–38], small clinical and biophysical differences with respect to the native protein were reported, and sometimes with discrepancies among the assays. While Rall et al. found reduced efficiency to activate LCAT of isolated K107del *in vitro* [39], this function was shown similar to Wt in other studies [40,41]. In a similar trend, lipid-binding affinity was reported either decreased [40], or similar to Wt [42]. Cholesterol efflux from cultured cells was not significantly altered by the deletion [43,44]. In other patients this mutant was associated with hypertriglyceridemia [38], and *in vitro* studies supported an increased binding to triglyceride-rich particles [42]. These findings suggest that, in addition to the lower efficiency that the mutation may induce in the normal apoA-I functions, the effect does not seem to be drastic. Instead, Wt protein that is also present in heterozygote subjects with a dissimilar prevalence of the mutated over the normal allele in all affected individuals may counterbalance minor shifts, which could explain -at least in part- the variety in the patients observations.

Here we first tested the hypothesis that the lack of the positive residue in position 107 induces a structural shift affecting protein folding and function. In accordance with previous reports [32,42], our data support a more flexible structure induced by the deletion. The lower efficiency of inter-chain crosslinking at concentrations greater than 0.1 mg/mL (Fig. 2A) may indicate a tridimensional protein folding that is more relaxed than Wt. In agreement with this, a small amount of Wt dimer could be detected in the Mass Spec analysis (inset in Fig. 4A) which is absent for the deletion mutant. The small red shift in the intrinsic Trp fluorescence of K107del shown here and the increased binding to ANS and Bis-ANS probes previously reported [19] also support a more flexible structure of the monomeric conformation.

Based on the class A model of alpha helices, Lys 107 should occur in a segment of the repeating 22-residue amphiphilic helices [45]. The traditional helix wheel simulations predict that the deletion of this residue induces a $\sim 90^{o}$ shift of helix axe, disrupting the nature and orientation of the hydrophobic face [39]. More recently, analysis based on the reported crystallographic structure of the C-terminal truncated apoA-I [46] suggested that this mutation would induce a weakening of the salt bridge networks [42]. To better strength this observation, we modeled and compared Wt and K107del by the SWISS MODEL predictor. As Fig. 6 suggests, a less compact domain might be generated due to the absence of that residue. Whether one or all the models predict the effect of the mutation is not known and must be further studied.

Despite the observed structural shift, neither lipid solubilization nor leakage of vesicles is significantly affected by the mutation. As the structural framework adopted by synthetic HDL was shown to closely resemble that of particles isolated *in vivo* [47] we intended to characterize the product of the interactions of the variants with DMPC (Suppl Fig. 2). It may be hypothesized that the mutation disrupts the natural arrangement of apoA-I impacting on HDL functionality. In this regard, it was proposed that the two molecules of apoA-I may adopt different registries within the particles [48,49] but the most efficient LCAT activation requires its interaction with a hybrid epitope involving the 6/4 helices of apoA-I of the two antiparallel molecules [49]. This hypothesis is supported by the finding that natural or artificial mutants in helices 4 (as it is the case of Lys107), or helices 5 or 6 show impaired LCAT activation [39]. In our hands, the product of the rearrangement of Lys107del with DMPC did not drastically differ from the Wt, which is in agreement with reports showing minor perturbations in the cholesterol efflux [43]. However, this fact does not preclude that under special conditions (probably lower lipid-to-protein ratios or other lipid compositions) the abnormalities in lipoprotein migration detected in some patients may be manifested. As Cooke et al. proposed, there might be a "a thumbwheel-like" mechanism of apoA-I on HDL particles, depending on particle lipid composition and diameter that may shift the helical registry [49].

The finding of dysfunctional HDL and apoA-I in the atherosclerosis plaque suggests that the protein may be a *victim* of the pro-inflammatory scenario. As we herein show, lipid function under intramolecular crosslinking is impaired being Wt more restrained from lipid solubilization than K107del (Fig. 5). In concordance with previous reports [32], the higher flexibility of K107del lipid-free protein may allow its reorganization as recruiting lipids even under some structural restraints following crosslinking. It remains to be determined if this effect on K107del is caused by crosslinking of non-crucial residues involved in the interaction with lipid domains or due to the major flexibility of mutant allowing to uncrosslink flexible-key domains (helices) to form the belt in discoidal HDL. In order to confirm this, specific experiments remain to be carried out in order to review the role of the amino group in position 107.

In addition to croslinking, another critical post translational modification is worth to be considered such as oxidation. In this trend we first set to analyze the probable loss in the efficiency of lipid solubilization. Instead, an increase in lipid binding affinity is observed as Wt

(and similarly observed for K107del) is oxidized under our experimental conditions, which is in accordance with Panzenböck observations on Wt [50]. The reasons for this behavior are not known but, as they suggest, it may be hypothesized that the introduction of a negative charge (sulfoxide groups) in the place of non polar Met at the boundary between a polar and non-polar faces may alter lipid-binding affinity [50]. In this trend, we have recently reported a similar behavior as the non-polar Leu was substituted by a polar Arg [51].

Oxidation may also affect protein native folding. A loss in the capacity to acquire a functional dimer conformation (as shown in Fig. 2C) or a higher tendency to aggregate of the oxidized variant may induce not only the impairment in protein function, but in addition to yield a cytotoxic species that could worsen the pro-inflammatory scenario. In this regard, we have recently shown that oxidized K107del is more sensitive than Wt to yield amyloid fibrils which elicit neutrophils activation [19].

As a conclusion, we suggest that it is required a drastic protein processing within the microenvironment, probably due to oxidations, crosslinkings, or both processes synergizing to induce a collapse of protein structure. This might be associated with either the loss of protein function (as lipid-binding), or its aggregation as amyloid complexes.

Author contribution statement

RAG and IDL performed the experiments, did data analysis and designed the research; HAG did data analysis and searched for funding, MCG did data analysis and discussed results, NAR and MAT designed the research, wrote the manuscript and searched for funding.

Declaration of Competing Interest

The authors declare that they have no known competing financial interests or personal relationships that could have appeared to influence the work reported in this paper.

Acknowledgements

Authors acknowledge Mr. Mario Ramos for invaluable help with figure design, Mrs. Rosana del Cid for English assistance and Miss Letizia Bauzá for expert contributions with size exclusion chromatography assays. This work was supported by the Consejo Nacional de Investigaciones Científicas y Técnicas (CONICET, PUE 22920160100002 to HG); Agencia Nacional de Promoción Científica y Tecnológica (ANPCyT, PICT-2016-0849 to MAT and PICT-2016-0915 to HG); Universidad Nacional de La Plata (UNLP) (M187 and M234 to MAT, PPID M014 to NAR).

Appendix A. Supplementary data

Supplementary data to this article can be found online at https://doi.org/10.1016/j.bbagen.2020.129732.

References

[1] J.F. Desforges, D.J. Gordon, B.M. Rifkind, High-density lipoprotein — the clinical implications of recent studies, N. Engl. J. Med. 321 (1989) 1311–1316, https://doi.org/10.1056/NEJM198911093211907.
[2] P.W.F. Wilson, R.D. Abbott, W.P. Castelli, High density lipoprotein cholesterol and mortality. The Framingham heart study, Arteriosclerosis 8 (1988) 737–741, https://doi.org/10.1161/01.atv.8.6.737.
[3] M. Cuchel, A. Rohatgi, F.M. Sacks, J.R. Guyton, JCL roundtable: high-density lipoprotein function and reverse cholesterol transport, J. Clin. Lipidol. (2018), https://doi.org/10.1016/j.jacl.2018.09.005.
[4] B.G. Drew, N.H. Fidge, G. Gallon-Beaumier, B.E. Kemp, B.A. Kingwell, High-density lipoprotein and apolipoprotein AI increase endothelial NO synthase activity by protein association and multisite phosphorylation, Proc. Natl. Acad. Sci. U. S. A. 101 (2004) 6999–7004, https://doi.org/10.1073/pnas.0306266101.
[5] W. Mu, M. Chen, Z. Gong, F. Zheng, Q. Xing, Expression of vascular cell adhesion molecule-1 in the aortic tissues of atherosclerotic patients and the associated clinical implications, Exp. Ther. Med. 10 (2015) 423–428, https://doi.org/10.3892/etm.2015.2540.
[6] P. Dimayuga, J. Zhu, S. Oguchi, K.-Y. Chyu, X.-O.H. Xu, J. Yano, P.K. Shah, J. Nilsson, B. Cercek, Reconstituted HDL containing human apolipoprotein A-1 reduces VCAM-1 expression and neointima formation following periadventitial Cuff-induced carotid injury in apoE null mice, Biochem. Biophys. Res. Commun. 264 (1999) 465–468, https://doi.org/10.1006/bbrc.1999.1278.
[7] V. González-Pecchi, S. Valdés, V. Pons, P. Honorato, L.O. Martinez, L. Lamperti, C. Aguayo, C. Radojkovic, Apolipoprotein A-I enhances proliferation of human endothelial progenitor cells and promotes angiogenesis through the cell surface ATP synthase, Microvasc. Res. 98 (2015) 9–15, https://doi.org/10.1016/j.mvr.2014.11.003.
[8] M. Ouimet, T.J. Barrett, E.A. Fisher, HDL and reverse cholesterol transport: basic mechanisms and their roles in vascular health and disease, Circ. Res. 124 (2019) 1505–1518, https://doi.org/10.1161/CIRCRESAHA.119.312617.
[9] S. Kopprasch, J. Pietzsch, J. Graessler, The protective effects of HDL and its constituents against neutrophil respiratory burst activation by hypochlorite-oxidized LDL, Mol. Cell. Biochem. 258 (2004) 121–127, https://doi.org/10.1023/B:MCBI.0000012842.19059.c5.
[10] M.F. Henning, V. Herlax, L. Bakás, Contribution of the C-terminal end of apolipoprotein AI to neutralization of lipopolysaccharide endotoxic effect, Innate Immun. 17 (2011) 327–337, https://doi.org/10.1177/1753425910370709.
[11] Y. Jie Yan, Y. Li, B. Lou, M. Ping Wu, Beneficial effects of ApoA-I on LPS-induced acute lung injury and endotoxemia in mice, Life Sci. 79 (2006) 210–215, https://doi.org/10.1016/j.lfs.2006.02.011.
[12] D.J. Rader, A.R. Tall, The not-so-simple HDL story: is it time to revise the hdl cholesterol hypothesis? Nat. Med. 18 (2012) 1344–1346, https://doi.org/10.1038/nm.2937.
[13] Y. Huang, J.A. Didonato, B.S. Levison, D. Schmitt, L. Li, Y. Wu, J. Buffa, T. Kim, G.S. Gerstenecker, X. Gu, C.S. Kadiyala, Z. Wang, M.K. Culley, J.E. Hazen, A.J. Didonato, X. Fu, S.Z. Berisha, D. Peng, T.T. Nguyen, S. Liang, C.-C.C. Chuang, L. Cho, E.F. Plow, P.L. Fox, V. Gogonea, W.H.W.W. Tang, J.S. Parks, E.A. Fisher, J.D. Smith, S.L. Hazen, An abundant dysfunctional apolipoprotein A1 in human atheroma, Nat. Med. 20 (2014) 193–203, https://doi.org/10.1038/nm.3459.
[14] J.A. DiDonato, Y. Huang, K.S. Aulak, O. Even-Or, G. Gerstenecker, V. Gogonea, Y. Wu, P.L. Fox, W.H.W. Tang, E.F. Plow, J.D. Smith, E.A. Fisher, S.L. Hazen, Function and distribution of apolipoprotein A1 in the artery wall are markedly distinct from those in plasma, Circulation. 128 (2013) 1644–1655, https://doi.org/10.1161/CIRCULATIONAHA.113.002624.
[15] G.I. Mucchiano, L. Jonasson, E. Einarsson, P. Westermark, Apolipoprotein A-I–Derived Amyloid in Atherosclerosis, (2001), pp. 298–303.
[16] L. Li, D. Cao, D.W. Garber, H. Kim, K.I. Fukuchi, Association of Aortic Atherosclerosis with cerebral β-amyloidosis and learning deficits in a mouse model of Alzheimer's disease, Am. J. Pathol. 163 (2003) 2155–2164, https://doi.org/10.1016/S0002-9440(10)63572-9.
[17] M. Eriksson, S. Schönland, S. Yumlu, U. Hegenbart, H. Von Hutten, Z. Gioeva, P. Lohse, J. Büttner, H. Schmidt, C. Röcken, Hereditary apolipoprotein AI-associated amyloidosis in surgical pathology specimens: identification of three novel mutations in the APOA1 gene, J. Mol. Diagn. 11 (2009) 257–262, https://doi.org/10.2353/jmoldx.2009.080161.
[18] M. Amarzguioui, G. Mucchiano, B. Häggqvist, P. Westermark, A. Kavlie, K. Sletten, H. Prydz, Extensive intimal apolipoprotein A1-derived amyloid deposits in a patient with an apolipoprotein A1 mutation, Biochem. Biophys. Res. Commun. 242 (1998) 534–539, https://doi.org/10.1006/bbrc.1997.8005.
[19] R.A. Gisonno, E.D. Prieto, J.P. Gorgojo, L.M. Curto, M.E. Rodriguez, S.A. Rosú, G.M. Gaddi, G.S. Finarelli, M.F. Cortez, G.R. Schinella, M.A. Tricerri, N.A. Ramella, Fibrillar conformation of an apolipoprotein A-I variant involved in amyloidosis and atherosclerosis, Biochim. Biophys. Acta - Gen. Subj. 2020 (1864), https://doi.org/10.1016/j.bbagen.2020.129515.
[20] E.D. Prieto, N. Ramella, L.A. Cuellar, M.A. Tricerri, H.A. Garda, Characterization of a human apolipoprotein A-I construct expressed in a bacterial system, Protein J. 31 (2012) 681–688, https://doi.org/10.1007/s10930-012-9448-z.
[21] N.A. Ramella, O.J. Rimoldi, E.D. Prieto, G.R. Schinella, S.A. Sanchez, M.E. Jaureguiberry, M.S. Vela, S.T. Ferreira, M.A. Tricerri, Human apolipoprotein A-I-derived amyloid: its association with atherosclerosis, PLoS One 6 (2011), https://doi.org/10.1371/journal.pone.0022532.
[22] K.A. Mcguire, W.S. Davidson, High Yield Overexpression and Characterization of Human Recombinant Proapolipoprotein A-L, 37, (1996).
[23] A. Krishnamoorthy, N. Tavoosi, G.K.L. Chan, J. Liu, G. Ren, G. Cavigiolio, R.O. Ryan, Effect of curcumin on amyloid-like aggregates generated from methionine-oxidized apolipoprotein A-I, FEBS Open Bio. 8 (2018) 302–310, https://doi.org/10.1002/2211-5463.12372.
[24] S.A. Rosú, O.J. Rimoldi, E.D. Prieto, L.M. Curto, J.M. Delfino, N.A. Ramella, M.A. Tricerri, Amyloidogenic propensity of a natural variant of human apolipoprotein A-I: stability and interaction with ligands, PLoS One 10 (2015), https://doi.org/10.1371/journal.pone.0124946.
[25] J. Wilschut, N. Düzgüneş, R. Fraley, D. Papahadjopoulos, Studies on the mechanism of membrane fusion: kinetics of calcium ion induced fusion of phosphatidylserine vesicles followed by a new assay for mixing of aqueous vesicle contents, Biochemistry. 19 (1980) 6011–6021, https://doi.org/10.1021/bi00567a011.
[26] A. Tricerri, B. Córsico, J.D. Toledo, H.A. Garda, R.R. Brenner, Conformation of apolipoprotein AI in reconstituted lipoprotein particles and particle-membrane interaction: effect of cholesterol, Biochim. Biophys. Acta - Lipids Lipid Metab. 1391 (1998) 67–78, https://doi.org/10.1016/S0005-2760(97)00187-2.

[27] L. Bordoli, F. Kiefer, K. Arnold, P. Benkert, J. Battey, T. Schwede, Protein structure homology modeling using SWISS-MODEL workspace, Nat. Protoc. 4 (2009) 1–13, https://doi.org/10.1038/nprot.2008.197.
[28] J.T. Melchior, R.G. Walker, A.L. Cooke, J. Morris, M. Castleberry, T.B. Thompson, M.K. Jones, H.D. Song, K.A. Rye, M.N. Oda, M.G. Sorci-Thomas, M.J. Thomas, J.W. Heinecke, X. Mei, D. Atkinson, J.P. Segrest, S. Lund-Katz, M.C. Phillips, W.S. Davidson, A consensus model of human apolipoprotein A-I in its monomeric and lipid-free state, Nat. Struct. Mol. Biol. 24 (2017) 1093–1099, https://doi.org/10.1038/nsmb.3501.
[29] E.F. Pettersen, T.D. Goddard, C.C. Huang, G.S. Couch, D.M. Greenblatt, E.C. Meng, T.E. Ferrin, UCSF chimera - a visualization system for exploratory research and analysis, J. Comput. Chem. 25 (2004) 1605–1612, https://doi.org/10.1002/jcc.20084.
[30] M.M. Bradford, A rapid and sensitive method for the quantitation of microgram quantities utilizing the principle of …, Anal. Biochem. 72 (1976) 248–254.
[31] W.S. Davidson, T. Hazlett, W.W. Mantulin, A. Jonas, The role of apolipoprotein AI domains in lipid binding, Proc. Natl. Acad. Sci. U. S. A. 93 (1996) 13605–13610, https://doi.org/10.1073/pnas.93.24.13605.
[32] N.A. Ramella, G.R. Schinella, S.T. Ferreira, E.D. Prieto, M. Vela, J.L. Ríos, M.A. Tricerri, O.J. Rimoldi, Human apolipoprotein A-I natural variants: molecular mechanisms underlying amyloidogenic propensity, PLoS One 7 (2012), https://doi.org/10.1371/journal.pone.0043755.
[33] G. Ponsin, A.M. Gotto, G. Utermann, H.J. Pownall, Abnormal interaction of the human apolipoprotein A-I variant [Lys107→0] with high density lipoproteins, Biochem. Biophys. Res. Commun. 133 (1985) 856–862, https://doi.org/10.1016/0006-291X(85)91213-6.
[34] G.K.L. Chan, A. Witkowski, D.L. Gantz, T.O. Zhang, M.T. Zanni, S. Jayaraman, G. Cavigiolio, Myeloperoxidase-mediated methionine oxidation promotes an amyloidogenic outcome for apolipoprotein A-I, J. Biol. Chem. 290 (2015) 10958–10971, https://doi.org/10.1074/jbc.M114.630442.
[35] Y.Q. Wong, K.J. Binger, G.J. Howlett, M.D.W. Griffin, Methionine oxidation induces amyloid fibril formation by full-length apolipoprotein A-I, Proc. Natl. Acad. Sci. 107 (2010) 1977–1982, https://doi.org/10.1073/pnas.0910136107.
[36] M. Tilly-Kiesi, A.H. Lichtenstein, J.M. Ordovas, G. Dolnikowski, R. Malmström, M.R. Taskinen, E.J. Schaefer, Subjects with Apoa-I(Lys107→0) exhibit enhanced fractional catabolic rate of ApoA-I in Lp(AI) and ApoA-II in Lp(AI with AII), Arterioscler. Thromb. Vasc. Biol. 17 (1997) 873–880, https://doi.org/10.1161/01.ATV.17.5.873.
[37] S. Ljunggren, J.H.M. Levels, M.V. Turkina, S. Sundberg, A.E. Bochem, K. Hovingh, A.G. Holleboom, M. Lindahl, J.A. Kuivenhoven, H. Karlsson, ApoA-I mutations, L202P and K131del, in HDL from heterozygotes with low HDL-C, Proteomics Clin. Appl. 8 (2014) 241–250, https://doi.org/10.1002/prca.201300014.
[38] J.R. Nofer, A. von Eckardstein, H. Wiebusch, W. Weng, H. Funke, H. Schulte, E. Köhler, G. Assmann, Screening for naturally occurring apolipoprotein A-I variants: apo A-I(ΔK107) is associated with low HDL-cholesterol levels in men but not in women, Hum. Genet. 96 (1995) 177–182, https://doi.org/10.1007/BF00207375.
[39] S.C. Rall, K.H. Weisgraber, R.W. Mahley, Y. Ogawa, C.J. Fielding, G. Utermann, J. Haas, A. Steinmetz, H.J. Menzel, G. Assmann, Abnormal lecithin: cholesterol acyltransferase activation by a human apolipoprotein A-I variant in which a single lysine residue is deleted, J. Biol. Chem. 259 (1984) 10063–10070.
[40] W. Huang, A. Matsunaga, W. Li, H. Han, A. Hoang, M. Kugi, T. Koga, D. Sviridov, N. Fidge, J. Sasaki, Recombinant proapoA-I(Lys107del) shows impaired lipid binding associated with reduced binding to plasma high density lipoprotein, Atherosclerosis. 159 (2001) 85–91, https://doi.org/10.1016/S0021-9150(01)00496-8.
[41] M. Tilly-Kiesi, Z. Qiuping, S. Ehnholm, J. Kahri, S. Lahdenpera, C. Ehnholm, M.R. Taskinen, ApoA-I(Helsinki) (Lys107→0) associated with reduced HDL cholesterol and LpA-I:A-II deficiency, Arterioscler. Thromb. Vasc. Biol. (1995), https://doi.org/10.1161/01.ATV.15.9.1294.
[42] I.N. Gorshkova, X. Mei, D. Atkinson, Binding of human apoA-I[K107del] variant to TG-rich particles: implications for mechanisms underlying hypertriglyceridemia, J. Lipid Res. 55 (2014) 1876–1885, https://doi.org/10.1194/jlr.m047241.
[43] M.C. Gonzalez, J.D. Toledo, M.A. Tricerri, H.A. Garda, The central type Y amphipathic α-helices of apolipoprotein AI are involved in the mobilization of intracellular cholesterol depots, Arch. Biochem. Biophys. 473 (2008) 34–41, https://doi.org/10.1016/j.abb.2008.02.021.
[44] A. Jonas, A. Von Eckardstein, L. Churgay, W.W. Mantulin, G. Assmann, Structural and functional properties of natural and chemical variants of apolipoprotein A-I, Biochim. Biophys. Acta (BBA)/Lipids Lipid Metab. 1166 (1993) 202–210, https://doi.org/10.1016/0005-2760(93)90098-T.
[45] J.P. Segrest, M.K. Jones, H. De Loof, C.G. Brouillette, Y.V. Venkatachalapathi, G.M. Anantharamaiah, The amphipathic helix in the exchangeable apolipoproteins: a review of secondary structure and function, J. Lipid Res. 33 (1992) 141–166 http://www.jlr.org/content/33/2/141.abstract.
[46] X. Mei, D. Atkinson, Crystal structure of C-terminal truncated apolipoprotein A-I reveals the assembly of high density lipoprotein (HDL) by dimerization, J. Biol. Chem. 286 (2011) 38570–38582, https://doi.org/10.1074/jbc.M111.260422.
[47] M.J. Thomas, S. Bhat, M. Sorci-Thomas, Three-dimensional models of HDL apoA-I: implications for its assembly and function, J. Lipid Res. 49 (2008) 1875–1883, https://doi.org/10.1194/jlr.R800010-JLR200.
[48] Y. He, H.D. Song, G.M. Anantharamaiah, M.N. Palgunachari, K.E. Bornfeldt, J.P. Segrest, J.W. Heinecke, Apolipoprotein A1 forms 5/5 and 5/4 antiparallel dimers in human high-density lipoprotein, Mol. Cell. Proteomics 18 (2019) 854–864, https://doi.org/10.1074/mcp.RA118.000878.
[49] A.L. Cooke, J. Morris, J.T. Melchior, S.E. Street, W. Gray Jerome, R. Huang, A.B. Herr, L.E. Smith, J.P. Segrest, A.T. Remaley, A.S. Shah, T.B. Thompson, W. Sean Davidson, A thumbwheel mechanism for APOA1 activation of LCAT activity in HDL, J. Lipid Res. 59 (2018) 1244–1255, https://doi.org/10.1194/jlr.M085332.
[50] U. Panzenböck, L. Kritharides, M. Raftery, K.A. Rye, R. Stocker, Oxidation of methionine residues to methionine sulfoxides does not decrease potential anti-atherogenic properties of apolipoprotein A-I, J. Biol. Chem. 275 (2000) 19536–19544, https://doi.org/10.1074/jbc.M000458200.
[51] G.M. Gaddi, R.A. Gisonno, S.A. Rosú, L.M. Curto, E.D. Prieto, G.R. Schinella, G.S. Finarelli, M.F. Cortez, L. Bauzá, E.E. Elías, N.A. Ramella, M.A. Tricerri, Structural analysis of a natural apolipoprotein A-I variant (L60R) associated with amyloidosis, Arch. Biochem. Biophys. 685 (2020), https://doi.org/10.1016/j.abb.2020.108347.